



# OPEN RAB13 regulates macrophage polarization in sepsis

Qingliang Zhu<sup>1,6</sup>, Dexiu Chen<sup>2,6</sup>, Shilin Li<sup>4</sup>, Wei Xiong<sup>5</sup>, Xianying Lei<sup>2</sup>, Wei Liu<sup>3✉</sup> & Yingchun Hu<sup>4✉</sup>

To select the core target (*RAB13*) in sepsis patients' peripheral blood and investigate its molecular functions and possible mechanisms. The peripheral blood of sepsis patients ( $n = 21$ ) and healthy individuals ( $n = 9$ ) within 24 h after admission were collected for RNA-seq, and differential gene screening was performed by iDEP online analysis software ( $P < 0.01$ ;  $\log_2FC \geq 2$ ) and enrichment analysis, the potential core target *RAB13* was screened out. The association between *RAB13* expression and sepsis severity was explored using multiple datasets in the GEO database, and survival analysis was conducted. Subsequently, peripheral blood mononuclear cells (PBMCs) from sepsis and control groups were isolated, and  $10 \times$  single-cell sequencing was used to identify the main *RAB13*-expressing cell types. Finally, LPS was used to stimulate THP1 cells to construct a sepsis model to explore the function and possible mechanism of *RAB13*. We found that *RAB13* was a potential core target, and *RAB13* expression level was positively associated with sepsis severity and negatively correlated with survival based on multiple public datasets. A single-cell sequencing indicated that *RAB13* is predominantly localized in monocytes. Cell experiments validated that *RAB13* is highly expressed in sepsis, and the knockdown of *RAB13* promotes the polarization of macrophages towards the M2 phenotype. This mechanism may be associated with the ECM-receptor interaction signaling pathway. The upregulation of *RAB13* in sepsis patients promotes the polarization of M2-like macrophages and correlates positively with the severity of sepsis.

**Keywords** Sepsis, RAB13, Macrophage polarization, ECM-receptor interaction

Sepsis is a globally prevalent disease. Although progress has been made in sepsis prevention and treatment, the mortality of septic shock remains high, reaching 35–40%<sup>1</sup>. Sepsis is an inflammatory condition caused by dysregulated host responses to pathogens, leading to organ failure, accompanied by immune disorder<sup>2</sup>. As an indispensable component of innate immunity, macrophages are principal natural immune cells and antigen-transporting cells with high plasticity. They can regulate the host's immune responses via differentiation and polarization, forming a multidimensional spectrum<sup>3</sup>. Macrophage polarization plays a significant role in sepsis prognosis<sup>4</sup>. Monocytes transform into macrophages after pathogen stimulation, and macrophages polarize into two phenotypic spectrums, M1- and M2-like. M1-like macrophages release copious inflammatory cytokines to induce cytokine storm syndrome and septic shock. M2-like macrophage-induced anti-inflammatory factors can effectively arrest sepsis progression<sup>5</sup>.

RAB GTPases are primary regulators of intracellular membrane transport and are involved in almost all steps in transportation, including vesicle formation, transport, and fusion<sup>6</sup>. *RAB13* is one of the Rab family members of small GTPases<sup>7</sup>, located at the human chromosome 12q13<sup>8</sup>. The protein encoded by *RAB13* is expressed on polarized epithelial cells, intestinal tract cells, endothelial cells, small intestinal epithelia, trophoblast cells, and blood-testis barrier-supporting cells. Additionally, the protein participates in the trafficking of tight junction protein occludin and tight junction protein-1 antibodies into tight junctions between epithelial cells<sup>9</sup> and regulates the membrane trafficking between the trans-Golgi network and recycling endosomes<sup>10</sup>. It was reported that *RAB13* can regulate the dynamic change of the specialized connecting structure between testicular supporting cells and spermatogenic cells, affecting physiological activities like sperm release<sup>11</sup>. Besides, *RAB13*'s role in tumors was extensively explored, showing that *RAB13* was upregulated in most cancers, such as breast cancer<sup>12</sup>,

<sup>1</sup>Department of Gastroenterology, The Affiliated Hospital, Southwest Medical University, Luzhou 646000, Sichuan, China. <sup>2</sup>Department of Critical Care Medicine, The Affiliated Hospital, Southwest Medical University, Luzhou 646000, Sichuan, China. <sup>3</sup>Department of Rheumatology and Immunology, The Affiliated Hospital, Southwest Medical University, Luzhou 646000, Sichuan, China. <sup>4</sup>Department of Emergency Medicine, The Affiliated Hospital, Southwest Medical University, Luzhou 646000, Sichuan, China. <sup>5</sup>Department of Emergency Medicine, The Leshan People's Hospital, Leshan 614000, Sichuan, China. <sup>6</sup>These authors contributed equally: Qingliang Zhu and Dexiu Chen. ✉email: liuweir244@sw.edu.cnmu; huyingchun913@swmu.edu.cn

glioma<sup>13</sup>, lymphoma<sup>14</sup>, etc. Additionally, *RAB13* expression is usually negatively correlated with prognosis<sup>7</sup> since *RAB13* promotes cancer cell migration and metastasis<sup>15</sup>. *RAB13*'s role in sepsis is insufficiently explored, and *RAB13* was found to be upregulated<sup>16</sup> in sepsis patients via bioinformatic methods based on a database. However, its reliability, molecular functions, and mechanisms remain unclear. This study revealed that sepsis patients had high *RAB13* expression, and high *RAB13* expression indicated poor prognosis in sepsis patients. Moreover, this study explored the molecular function and potential mechanisms of *RAB13* in sepsis. Workflow of the project is displayed in Fig. 1.

## Methods and materials

### Sample collection

From December 2018 to 2019, we collected peripheral blood samples within 24 h of admission from 21 septic patients and 9 healthy controls admitted to the ICU/EICU of the Southwest Medical University Hospital, and the samples were stored in  $-80^{\circ}\text{C}$  freezers. The anticoagulation Tube utilizes the PAXgene<sup>®</sup> Blood RNA System (BD Biosciences), comprising the PAXgene<sup>®</sup> Blood RNA Tube and nucleic acid purification Kit (PAXgene<sup>®</sup> Blood RNA Kit). The PAXgene<sup>®</sup> Blood RNA tube contains an additive that enhances in vivo gene transcription profile stability by reducing in vitro RNA degradation and minimizing gene induction. Inclusion criteria: SEPSIS 3.0 criteria were used, infection was present, and qSOFA  $\geq 2$ . Exclusion criteria: (1) age below 16 years or above 65 years, (2) previous organ failure, (3) Patients with a previous history of immunodeficiency, (4) Patients who refused to be enrolled. All participants or their relatives signed informed consent, this trial passed the Ethics Committee of the Affiliated Hospital of Southwest Medical University (ethics number: ky2018029), and the clinical trial registration number: ChiCTR1900021261.

Whole blood samples were collected from patients with sepsis ( $n = 2$ ), patients with systemic inflammatory response syndrome (SIRS) ( $n = 1$ ), and healthy individuals ( $n = 2$ ) admitted to the ICU of Southwest Medical University Hospital within 24 h in April 2022, with the same inclusion and exclusion criteria for sepsis as above. SIRS inclusion criteria with the presence of at least two of the following four clinical criteria: (1) shortness of breath ( $> 20$  breaths/min or  $\text{PaCO}_2$  or  $< 4.3$  kPa (32 mmHg), or the need for mechanical ventilation; (2) fever or hypothermia (temperature  $> 38$  or  $< 36^{\circ}\text{C}$ ); (3) tachycardia ( $> 90$  beats/min); (4) altered white blood cell count ( $> 12,000$  cells/uL, or  $< 4000$  cells/uL, or presence of  $> 10\%$  band forms. All cases were signed by the patients or their relatives to ensure informed consent for inclusion in the study; this experiment passed the Ethics Committee of the Affiliated Hospital of Southwest Medical University (ethics number: ky2022094), and the clinical trial registration number is ChiCTR2200057401. The study has obtained the informed consent of all participants and/or their legal guardians. Studies involving human study participants are conducted in accordance with the Declaration of Helsinki.

### Peripheral blood gene sequencing and screening

Total RNA from peripheral blood samples was extracted using the Trizol method (Invitrogen, Carlsbad, CA, USA) and quantified using Agilent 2100 (Thermo Fisher Scientific, MA, USA). Ribosome RNA (rRNA) was removed using H reagents (Shanghai First Research Institute) that specifically target oligonucleotides and ribonucleases (RNase) following the manufacturer's instructions. Total RNA was purified using RNA-SPRI beads and fragmented into small pieces using divalent cations at high temperatures. The cleaved RNA fragments were copied into the first-strand cDNA using reverse transcriptase and random primers. Second-strand cDNA was

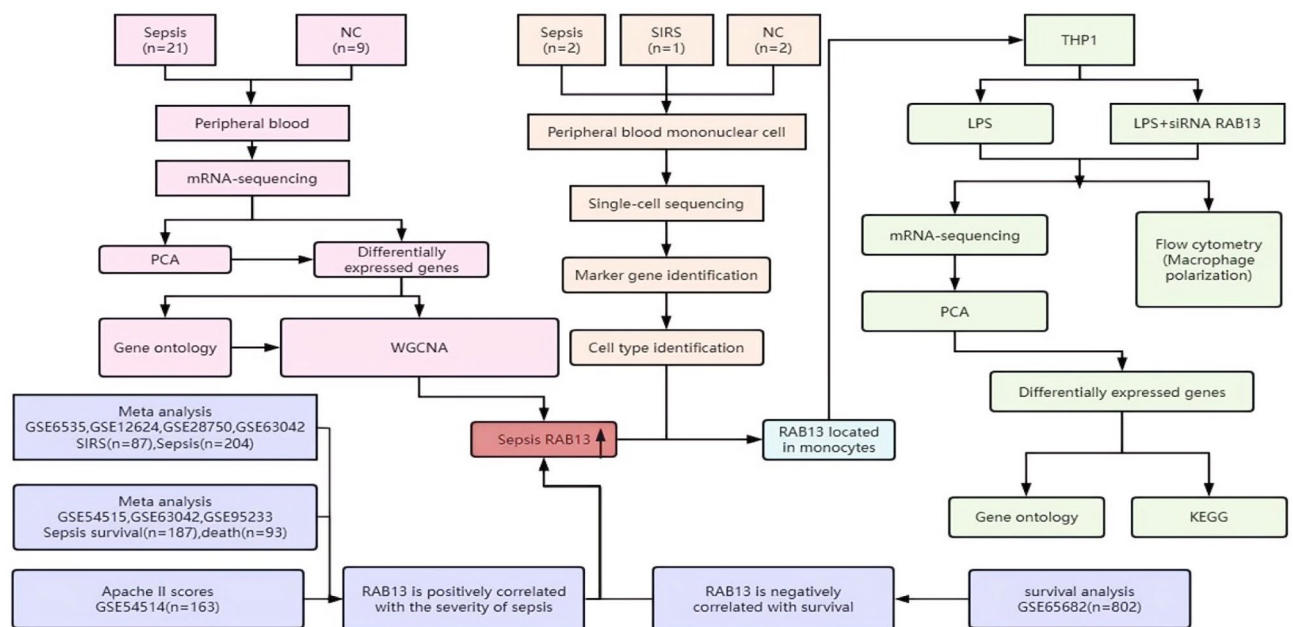


**Fig. 1.** Experimental flow chart of this study.

synthesized with DNA polymerase I and RNase H. The quality and quantity of libraries were evaluated using two methods: checking average fragment size distribution using Agilent 2100 bioanalyzer and quantifying libraries using quantitative real-time PCR (qRT-PCR, TaqMan Probe). Eligible libraries were subjected to paired-end sequencing using the BGISEQ-500/MGISEQ-2000 system (BGI-Shenzhen, China). Raw data for sequencing were first filtered using SOAPnuke (<https://github.com/BGI-flexlab/SOAPnuke>), and the Clean Reads were saved in the FASTQ format.

### DEG screening

Data matrixes were processed for normalized quality control (EdgeR:  $\log_2(\text{CPM} + 4)$ ) using the online analysis platform iDEP1.0 based on the R language. Outlier samples were excluded by dimension reduction analysis using the principal component analysis (PCA) method, and sample clusters with high similarity were identified. The statistical method was Deseq2, and DEGs were selected by comparing the two groups. Genes with  $P < 0.01$  and  $\log_2\text{FC} \geq 2$  were selected.

### Gene ontology (GO) analysis

Gene ontology (GO) analysis describes the functions of a particular gene in biological process (BP), cellular component (CC), and molecular function (MF). Here, GO annotation was performed for differently expressed mRNA (DEmRNA) to further investigate the functional enrichment of DEGs.  $P < 0.05$  was interpreted as statistically significant. This study focuses on specific ligand recipients or interactions between inflammatory mediators and recipients to explore intercellular communications.

### Weighted correlation network analysis (WGCNA)

Weighted correlation network analysis (WGCNA) defines genes with similar expression trends as modules. Those genes have similar expression variations in the same physiological process or different tissues, showing similarity or correlation in functions. Thus, this approach predicts the functions of some de novo genes or RNA. Here, a co-expression network was established using the iDEP1.0 online platform to screen hub genes involved in sepsis.

### Meta-analysis

Other sepsis datasets were downloaded from the GEO public database, and hub genes were validated using meta-analysis. Dataset screening criteria: (1) homo sapiens; (2) peripheral blood samples; (3) microarrays or RNA-seq; (4) age  $\geq 16$  years and  $\leq 65$  years; (5) sepsis patients as observation group and healthy people as the control group; (6) total sample size  $\geq 20$ . All primary data were processed for quality control, and datasets with poor quality were excluded. Eventually, GSE6535, GSE12624, GSE28750, GSE63042, GSE54514, and GSE95233 were obtained as high-quality datasets. When a gene corresponded to multiple values, we took the average value as the expression value of the gene. The expression of hub genes underwent meta-analysis with a Forest plot generated.

### Receiver operating characteristic (ROC) curve

Patients from the GSE28750, GSE67652, GSE69528, and GSE95233 datasets were divided into sepsis and control groups. The ROC curve was generated to assess the diagnostic accuracy of DEGs for sepsis using MedCalc.

### Survival analysis

To explore the prognostic significance of hub genes in sepsis patients, we downloaded the public dataset GSE65682, including the clinical data (gene expression data and survival) of 479 patients and 365 sepsis survivors. Patients were classified into high- and low-expression groups based on *RAB13* expression. The results were visualized using Prism9 (GraphPad) and examined using a log-rank test, and  $P < 0.05$  was defined as statistically significant.

### Single-cell sequencing

Five peripheral blood samples were collected (2 healthy controls, 1 SIRS sample, and 2 sepsis samples). PBMCs were obtained using Ficoll gradient centrifugation with  $10 \times$  Genomics conducted. The  $10 \times$  Genomics platform uses microfluidic technology to encapsulate beads and cells with Cell Barcode in droplets, collect the droplets containing the cells, and then lyse the cells in the droplets so that the mRNA in the cells binds to the Cell Barcode on the beads to form Single Cell GEMs, in which reverse transcription reactions are performed to construct cDNA libraries, which are sampled on the library sequences Distinguish the sample source of the target sequence. Raw reads generated from high-throughput sequencing were in fastq format, processed using  $10 \times$  Genomics software CellRanger, and further analyzed with the Seurat package. Gene expression was subjected to PCA for linear dimension reduction with results visualized via tSNE (non-linear dimensional reduction). In addition, gene markers were identified using the FindAllMarkers function, and identified genes were visualized via VlnPlot and FeaturePlot functions.

### Cell culture and modeling

Human-derived THP-1 cells (Procell CL-0233, China) were selected to construct sepsis cellular models. THP-1 cells were cultured in complete mediums (RPMI-1640 supplemented (Supplementary Material) with 10% FBS, 1% P/S solution, and 0.05 mM  $\beta$ -mercaptoethanol) and maintained in 5%  $\text{CO}_2$  at 37 °C. Subsequently, samples were treated with PMA (50 ng/ml) for 48 h, and THP-1 cells were coaxed into M0 macrophages. After resting overnight, cells were stimulated with 100 ng/ml lipopolysaccharides (LPS) for 6 h to establish sepsis models, while the normal group was given medium replacement alone<sup>17,18</sup>.

### siRNA transfecting THP-1 cells

Human THP-1 cells were grouped: (1) control group: no treatment after cells adhering to the walls; (2) LPS group: sepsis model group: LPS stimulation for 24 h; (3) LPS + *RAB13* group: sepsis models were constructed with cells with *RAB13* knockdown. Opti-MEM reduced serum medium was used with Lipofectamine 8000 transfecting reagent (Life Technologies). siRNA sequences were selected via experiments: UUAUUGUCUUGAACCGCU CTT. siRNA was dissolved. The day before transfection, cells were inoculated into a 6-well plate at  $3.0 \times 10^5$  cells per well with 2 mL of growth medium added into each well. Before transfection, the original mediums were replaced with fresh mediums (2 mL, complete mediums containing Human serum and antibiotics). Subsequently, Add 125  $\mu$ L Opti-MEM<sup>®</sup> medium, 100 pmol siRNA, 4  $\mu$ L transfection reagent, gently mix by pipetting, and incubate at room temperature for 20 min. After changing the complete mediums, the plate was placed in a 37 °C incubator for 24 h.

### RT-qPCR

Total RNA was extracted using the Total RNA extraction kit (DEPC Takara, Japan), and the concentration and purity were measured with a spectrophotometer (Beijing Kaiuo Technology Development Co., LTD K5600). RNA was reverse-transcribed into cDNA using the PrimeScript RT reagent Kit with a gDNA Eraser (Takara, Japan). PCR process: 94 °C for 30 s; 40 cycles of 94 °C for 5 s, 60 °C for 30 s. Primer sequence: GAPDH-F; CAACGA CCCCTTCATTGACC; GAPDH-R CGCTCCTGGAAGATGGTGAT; *RAB13*-F CCAAAGCCTACGACCACC TC; *RAB13*-R AGTTGTCCTCTGCAAAGCGAA; GAPDH-F CAACGACCCCTTCATTGACC, GAPDH-R, CGCTCCTGGAAGATGGTGAT; Subsequently, PCR was performed using SYBR Green PCR Master Mix (NO. QPK-201, TOYOBO Co., Ltd, Japan) according to the manufacturer's protocols. Real-time monitoring of PCR reaction was conducted using a real-time thermal cycler (Analytik Jena AG, Germany). The results were analyzed using the  $2^{-\Delta\Delta Ct}$  method.

### Flow cytometry

Macrophage polarization was appraised by flow cytometry to differentiate M1- and M2-like macrophages. One day before transfection, cells were inoculated to a 6-well plate at  $3.0 \times 10^5$  cells/well with 2 mL of PMA (50 ng/mL) added into each well. 24 h later, growth medium (125  $\mu$ L) without antibiotics and serum, siRNA (100 pmol), and Lipo8000 transfection reagent (4  $\mu$ L) were added to the plate. Collect  $1 \times 10^6$  cells in a 2 mL EP tube, centrifuge at  $350 \times g$ , 4 °C for 5 min, and discard the supernatant. APC anti-human *CD86*<sup>19</sup> (5  $\mu$ L Biologend, 374207) and FITC anti-human *CD206*<sup>20</sup> (5  $\mu$ L, Biologend, 321103) were supplemented to the LPS and LPS + *RAB13* groups, respectively. Following twice PBS washing, cells were examined. *CD86* was used as a marker to detect M1 macrophages. *CD206* was used as a marker to detect M2 macrophages. Add 2 mL pre-cooled PBS to wash the cells, centrifuge at  $350 \times g$  for 5 min, and discard the supernatant. Repeat the previous step. Resuspend the cell pellet in 0.1 mL of cell staining buffer and analyze it on a flow cytometer (NovoCyte, ACEA).

### RNA-seq

THP1 cells from the LPS and LPS + *RAB13* groups underwent RNA-seq. First-strand cDNA was synthesized with M-MuLV reverse transcriptase using NEBNext<sup>®</sup> Ultra RNA Library Prep Kit for Illumina. Subsequently, RNA was degraded with RNaseH, and second-strand cDNA was synthesized with dNTPs in the DNA polymerase I system. Purified double-stranded cDNA underwent end repair, A-tailing, and adaptor ligation. Subsequently, cDNA was selected using AMPure XP beads. PCR amplification and PCR product purification were conducted to obtain the final library. RNA-seq data were analyzed by Qubit 2.0 and Agilent 2100.

### Statistical analysis

Standard variable data were expressed as mean  $\pm$  SD and analyzed using a t-test.  $P < 0.05$  was considered statistically significant. Raw RNA-seq data were compared following log transformation. The survival curve was analyzed using a log-rank test, and hub genes were validated by continuous variable meta-analysis. GraphPad Prism 9.0 (Graph Pad Inc., La Jolla, CA) was used to analyze data and plot diagrams.

## Results

### Baseline data results

We collected information including gender, age, white blood cell (WBC), procalcitonin (PCT), SOFA score, and data reflecting organ injury (direct bilirubin, creatinine, urea) from sepsis patients and healthy volunteers. The clinical data are shown in (Table 1). There was no statistically significant difference in age between the two groups. Compared with healthy individuals, inflammation indexes and SOFA scores were higher in sepsis patients, while GCS scores were lower.

### High *RAB13* expression in sepsis patients

Box mapping (Fig. 2a) and PCA analysis (Fig. 2b) for mRNA revealed that the two groups had close mean values. Thus, the two groups were comparable in discrimination. DEG screening ( $P < 0.01$ ;  $\log_2 FC \geq 2$ ) showed that sepsis patients had 1077 DEGs in the peripheral blood versus the control group, 725 genes were up-regulated, and 352 genes were down-regulated (Fig. 2c). GO and KEGG analyses indicated that those DEGs were primarily enriched in external encapsulating structure organization, extracellular structure organization, extracellular matrix organization, specific granule, tertiary granule, specific granule lumen, glycosaminoglycan binding, immune receptor activity, heparin-binding transcriptional misregulation in cancer, complement and coagulation

Clinic items	Sepsis (n=21)	NC (n=9)	p
Gender (F/M)	8/13	4/5	–
Age (years)	58.2 ± 2.52	53.44 ± 3.63	0.899
SOFA	5.86 ± 0.60	0 ± 0	0.0001
GCS	11.1 ± 0.89	15 ± 0	0.0001
WBC(10 <sup>9</sup> /L)	11.87 ± 1.756	6.26 ± 0.607	0.003
NEU(10 <sup>9</sup> /L)	10.2 ± 1.531	3.71 ± 0.461	0.001
TBIL(umol/L)	53.87 ± 23.45	14.62 ± 1.56	0.81
Urea(mmol/L)	9.64 ± 1.728	5.44 ± 0.528	0.137
Cre(umol/L)	129.62 ± 35.708	69.38 ± 3.849	0.116

**Table 1.** Demographic and clinical data of subjects (m ± sd). Gender, age, SOFA score, glasgow coma scale (GCS) score, total white blood cell (WBC) count, neutrophil count, total bilirubin, urea, and serum creatinine.

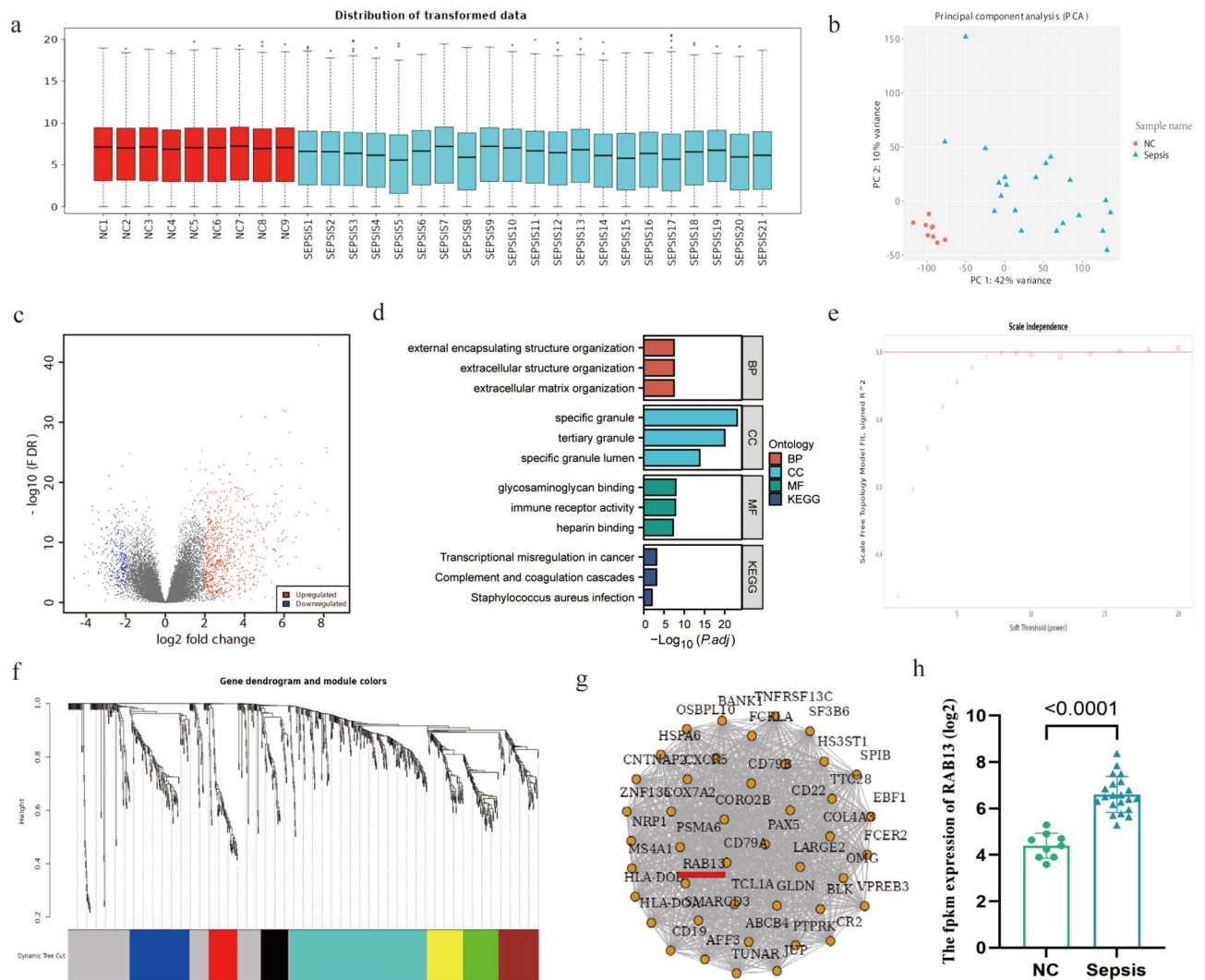


**Fig. 2.** Bioinformatics analysis of RNA-seq data. (a) Box plot of sepsis and NC samples. (b) PCA of mRNAs. (c) Volcano plot of mRNAs (fold-change ≥ 2.0, FDR < 0.01). (d) The results of gene ontology analysis and KEGG. (e) WGCNA Soft threshold = 8. (f) The turquoise module exhibits a high correlation with the clinical features of sepsis. (g) Modules based on the topological overlap of mRNA co-expression in the turquoise module (module size > 50). (h) The fpkm expression of RAB13 (log<sub>2</sub>) between normal and sepsis groups.

cascades, staphylococcus aureus infection, etc. (Fig. 2d). Potential core target *RAB13* was selected via WGCNA analysis (Fig. 2e–g). Sepsis patients had significantly elevated *RAB13* (Fig. 2h).

***RAB13* was positively correlated with sepsis severity**

The area under the curve (AUC) indicated that *RAB13* had high sensitivity and specificity (Fig. 3a–d). Based on dataset GSE54514, *RAB13* was shown to be positively correlated with patients’ Apache II scores (Fig. 3e). Meta-analysis suggested that sepsis patients had high *RAB13* expression versus the SIRS group (Fig. 3f), *RAB13* exhibits higher expression in the sepsis survival group compared to the non-survival group (Fig. 3g). Survival analysis revealed that *RAB13* was negatively associated with patients’ survival rates (Fig. 3h).

**Single-cell sequencing indicated that *RAB13* is predominantly localized in monocyte macrophages**

The single-cell sequencing flow is shown in the figure. (Fig. 4a). By identifying marker genes, 5 subsets were acquired: T cells, NK cells, monocytes, B cells, and platelets (PLT) (Fig. 4b). *CD2* and *CD3D* were regarded as T cell markers (Fig. 4c), and *CD163* and *LYZ* were regarded as “monocyte/macrophage” markers (Fig. 4d). Thus, *RAB13* was mainly expressed in monocytes/macrophages (Fig. 4e).

**Inhibition of *RAB13* expression promotes M2 macrophage polarization**

Examination of *RAB13* expression in various cell groups via RT-qPCR. Compared to the control group, the *RAB13* expression in the LPS group was significantly elevated. In contrast, compared to both the control and LPS groups, the *RAB13* expression in the siRNA group was markedly reduced. These differences were statistically significant ( $P < 0.05$ ) (Fig. 5a). *CD86* and *CD206* were used for M1 and M2 detection via Flow cytometry (Fig. 5b,c).

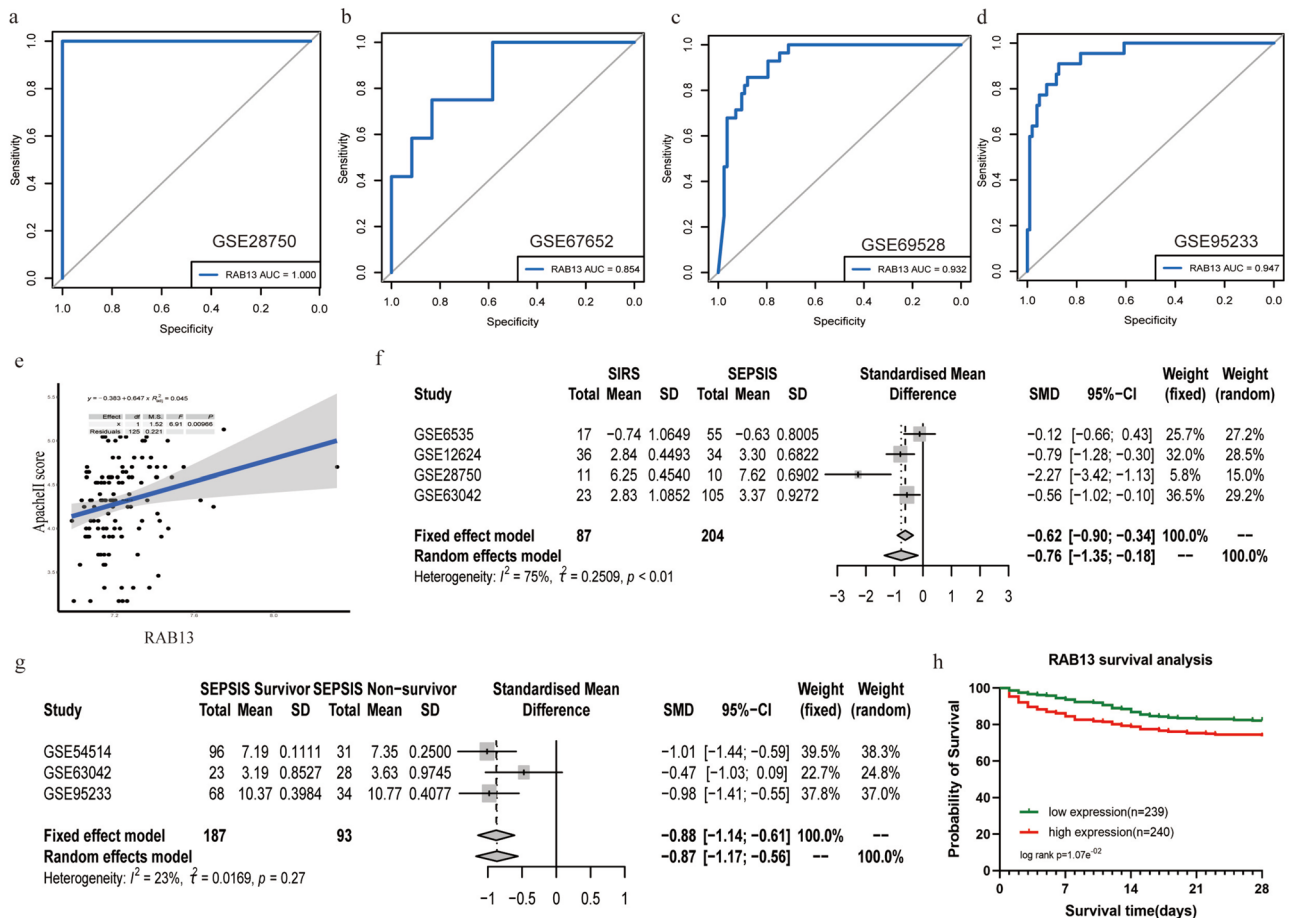


**Fig. 3.** Clinical significance of *RAB13*. (a–d) ROC curve of *RAB13* for the comparison between normal groups vs sepsis groups based on the data set GSE28750, GSE67652, GSE69528, GSE95233. (e) Based on the dataset GSE54514, *RAB13* expression levels were positively correlated with patients’ Apache II scores. (f) Meta-analysis of *RAB13* based on the GSE6535, GSE12624, GSE28750, and GSE63042 datasets showed that *RAB13* was higher in the sepsis group compared to the SIRS group. (g) *RAB13* meta-analysis based on the GSE54514, GSE63042, and GSE95233 datasets showed that *RAB13* expression was higher in the sepsis survival group than in the sepsis non-survival group. (h) Survival analysis of *RAB13* based on the dataset GSE65682 suggested that *RAB13* was negatively associated with patient survival.

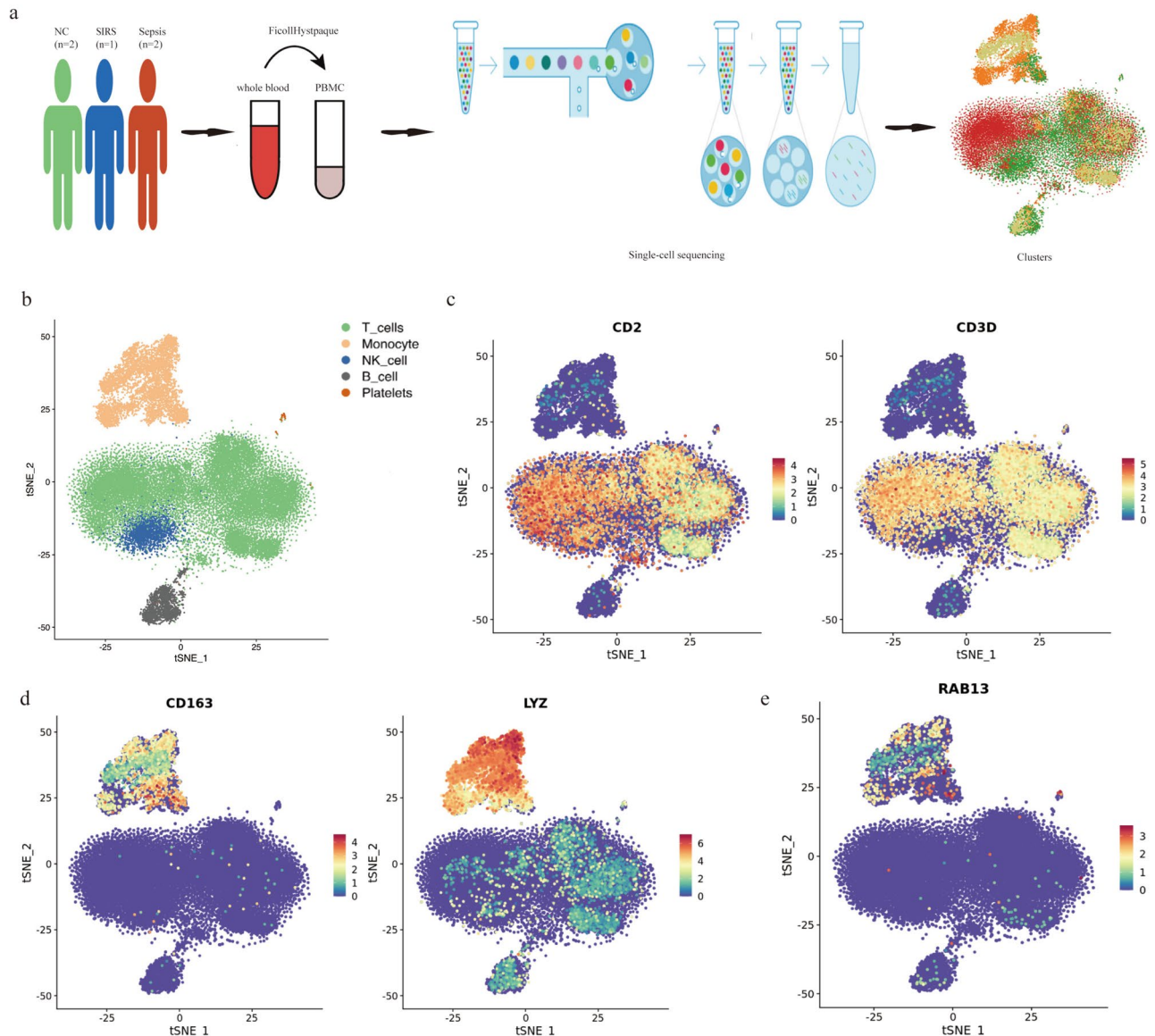


**Fig. 4.** Single cell RNA-Seq. **(a)** Single-cell RNA-seq process. **(b)** Five types of cell populations including macrophages, natural killer cells, T cells, B cells, and platelets were identified by marker genes. **(c)** *CD2* and *CD3D* are T-cell markers. **(d)** *CD163* and *LYZ* were regarded as monocyte/macrophage markers. **(e)** *RAB13* was mainly expressed in monocytes/macrophages.

After 24 h of modeling, the polarization of M1 and M2 macrophages was detected by flow cytometry. The results indicated that *RAB13* knockdown promoted the polarization of macrophages towards The M2 phenotype, without significantly affecting the polarization towards the M1 phenotype (Fig. 5d–f).

### ***RAB13* might promote M2 macrophage polarization via the ECM-receptor interaction signaling pathway**

To explore the potential molecular mechanism of *RAB13* inhibiting M2 macrophage polarization, we transfected human THP1 cells with *RAB13* siRNA and constructed sepsis models using LPS (100 ng/ml) stimulation 24 h later. RNA-seq analysis was performed 6 h later for THP1 cells in the LPS and LPS + *RAB13* groups. Following quality control, gene expression quantification, and standardization of sequencing data, the mean values of samples from the two groups were at the same level, and the two groups were comparable (Fig. 6a). By analyzing sample similarity, intragroup samples showed a high correlation (Fig. 6b). Altogether 1536 DEGs were selected from the two groups using  $|\log_2\text{-fold change}| > 2$  and  $\text{padj} < 0.01$ , 1334 genes were upregulated, and 202 genes were downregulated (Fig. 6c). GO and KEGG pathway analyses were conducted to explore the biological pathways and functions of DEGs. With False Discovery Rate (FDR)  $< 0.01$  and  $P < 0.05$  as the threshold, 27 GO terms were obtained (Fig. 6d). Cellular localization was mainly collagen-containing extracellular matrix, spanning components of the plasma membrane, microvillus membrane, etc. Biological processes were primarily correlated with response to lipopolysaccharides, cell adhesion, immune system process regulation, etc. Molecular functions were

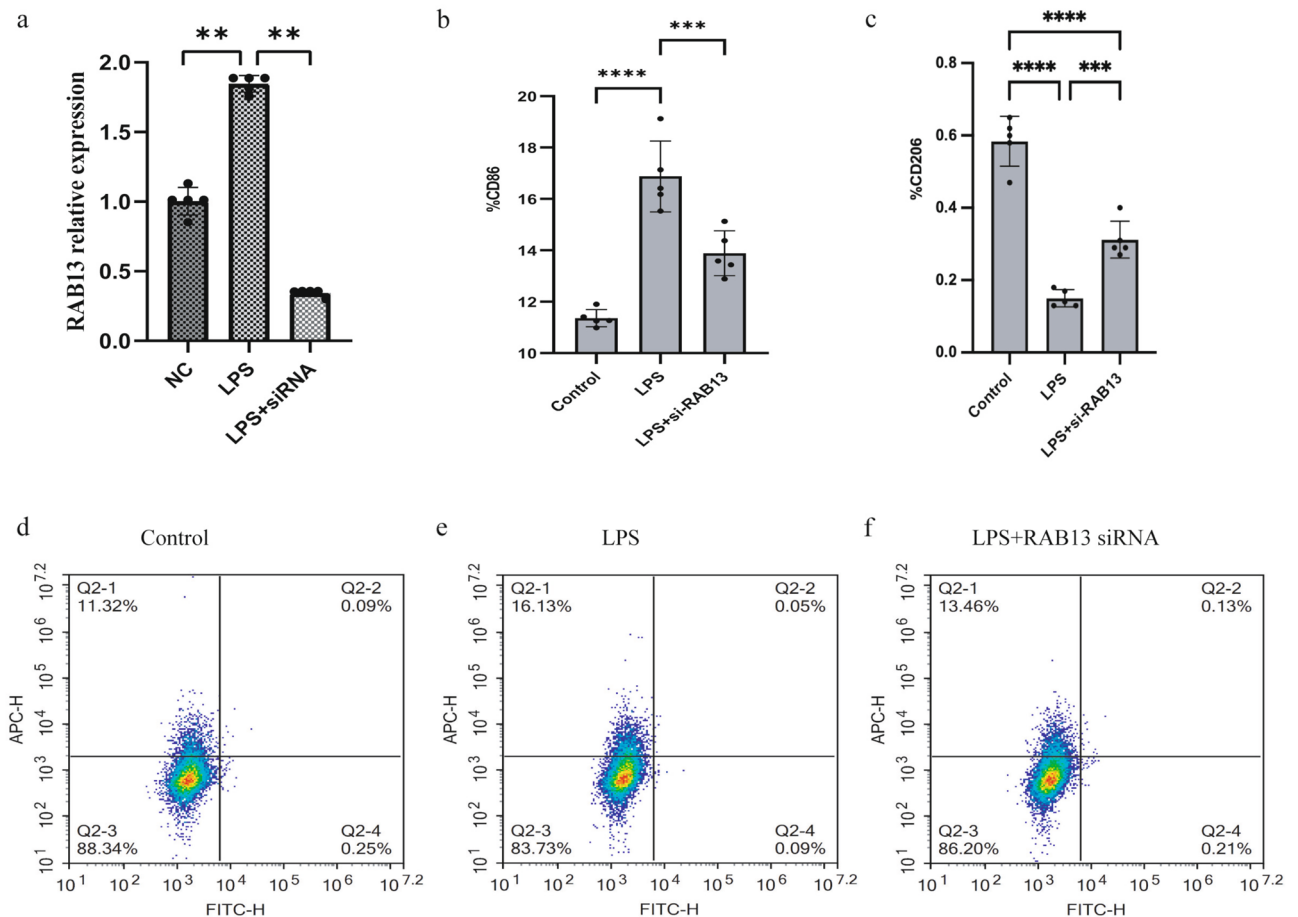


**Fig. 5.** The molecular function of *RAB13* was explored using the THP1 cell line. **(a)** Examination of *RAB13* expression in various cell groups via RT-qPCR. Compared to the control group, the *RAB13* expression in the LPS group was significantly elevated. In contrast, compared to both the control and LPS groups, the *RAB13* expression in the siRNA group was markedly reduced. **(b)** *CD86* was used as a marker to detect M1 macrophages. **(c)** *CD206* was used as a marker to detect M2 macrophages. **(d–f)** *RAB13* knockdown promotes M2 phenotype polarization in macrophages (\*\*\*\* $p < 0.0001$ ; \*\*\* $p < 0.001$ ; \*\* $p < 0.01$ ; \* $p < 0.05$ ).

mainly associated with chemokine activity and recipient binding, cytokine activity, etc. (FDR < 0.01,  $P < 0.05$ ). KEGG enrichment analysis demonstrated that enriched pathways were Cytokine-cytokine receptor interaction, Viral protein interaction with cytokine and cytokine receptor, Neuroactive ligand-receptor interaction, and ECM-receptor interaction signaling pathways (Fig. 6e).

## Discussion

There are over 18 million severe sepsis cases annually worldwide<sup>21</sup>. Although progress has been made in treatment, mortality remains high, for which insufficient early identification and inadequate understanding of the pathophysiological mechanisms are the primary causes. Hence, molecular markers for sepsis severity are urgently needed with molecular mechanisms pending to be explored, to provide a reference for sepsis treatment<sup>22</sup>.

RNA-seq analysis was conducted for peripheral blood samples of sepsis patients and healthy controls, showing that *RAB13* was highly expressed in sepsis patients as a potential core target, consistent with previous studies<sup>16</sup>. Validation was carried out using the GEO database, suggesting that *RAB13* had high sensitivity and specificity among multiple datasets as a potential molecular marker. Moreover, meta-analysis for multiple datasets indicated that *RAB13* was progressively elevated in SIRS, sepsis survival, and sepsis death groups. Combining clinical prognostic information, *RAB13* was illustrated to be positively correlated with the Apache II score and negatively related to the survival rate. In brief, *RAB13* was highly expressed in sepsis patients and positively associated with sepsis severity. Thus, *RAB13* can serve as a potential prognostic biomarker to identify sepsis severity and play a significant role in sepsis.

Under physical status, *RAB13* predominantly participates in membrane trafficking<sup>10</sup>, including post-Golgi trafficking<sup>23</sup>, Glut4 vesicle exocytosis<sup>24</sup>, etc. In tumors, *RAB13* can modulate autophagy<sup>25</sup>, and foster tumor cell migration and invasion<sup>6</sup>. Research has revealed that *RAB13* exhibits differential expression across various cancers, including liver hepatocellular carcinoma (LIHC) and Stomach Adenocarcinoma (STAD). It has been concluded that *RAB13* may serve as a potential therapeutic target for Liver Hepatocellular Carcinoma and can function as a prognostic biomarker<sup>26</sup>. *RAB13*'s role in sepsis is insufficiently explored. Previous studies have found that



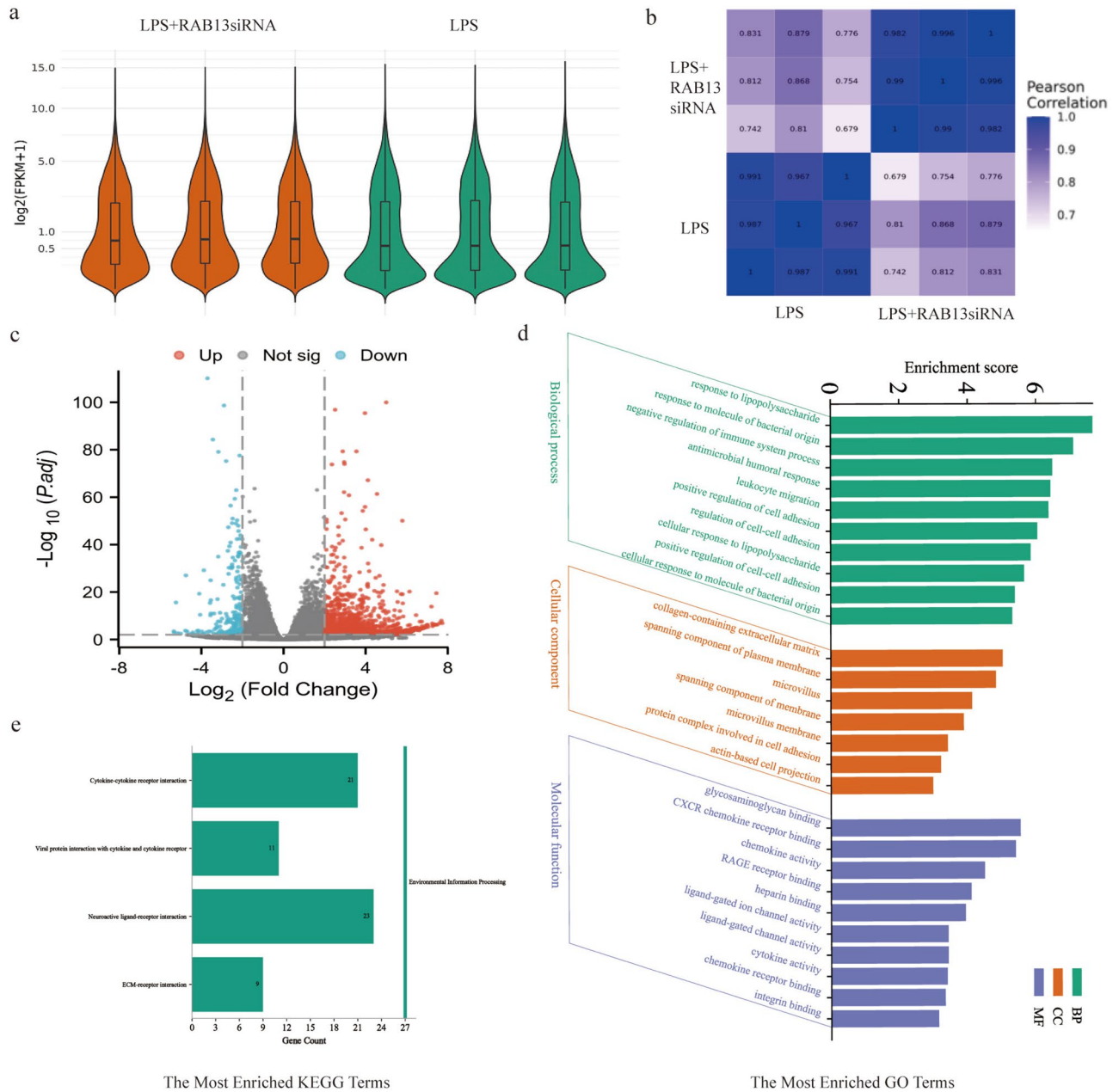


**Fig. 6.** *RAB13* was knocked down in the THP1 cell line and the possible molecular functional mechanism was analyzed by bioinformatics. (a) Box map of gene expression distribution. (b) Pearson similarity heat map. (c) Differential gene volcano map. (d) Histogram of GO enrichment results of differential genes. *BP* biological process, *CC* cellular component, *MF* molecular function. (e) Histogram of KEGG enrichment results of differential genes.

*RAB13* is involved in LPS-stimulated phagocytosis of macrophages<sup>15,27</sup>, and we found that *RAB13* was mainly localized to monocytes by single-cell sequencing of peripheral blood PBMCs from sepsis patients. Monocytes can differentiate into macrophages under stimulation. Macrophages have plasticity and diversity and can polarize toward the M1 or M2 phenotype in microenvironments. M1- and M2-type macrophages are not two independent categories but represent extremes along a continuum with overlaps. Thus, the two phenotypes can interconvert into each other in a certain microenvironment<sup>28–30</sup>. In the early stage of sepsis, pro-inflammatory cytokines in the host like interferon- $\gamma$  and LPS induce M1 macrophage polarization and release substantial inflammatory factors, such as *TNF- $\alpha$* , *IL-1 $\beta$* , and reactive oxygen species (ROS). M1-type macrophages present relatively strong cytotoxic activity, kill pathogens, clear aberrant endogenous tissue and cells in the immune microenvironment, and can injure tissue, organs, and immune cells. In the late stage of sepsis, an excessive increase of M2-type macrophages induces a considerable release of anti-inflammatory cytokines (e.g., *IL-10*). These cytokines can coax immunosuppression to mitigate inflammatory injuries and cause immune paralysis in the host, making the host susceptible to secondary infections<sup>3,5,31</sup>. Therefore, induction of macrophage polarization is a potential direction for sepsis treatment.

In this study, the cellular experiments revealed that the suppression of *RAB13* expression led to an increase in M2 macrophage polarization. Numerous literature sources indicate that inhibiting M1-like macrophage polarization aids in reducing organ dysfunction<sup>32,33</sup>. This observation appears to contradict the fact that patients with elevated *RAB13* levels in sepsis exhibit poorer outcomes. However, early inhibition of M1-like macrophage polarization and the release of pro-inflammatory factors during sepsis may also result in suppressed pathogen clearance, making infection control more challenging and potentially leading to even worse prognoses.

Macrophage polarization is realized through complicated gene networks and signaling cascades dynamically regulating multiple genes' expression. Transcription and translation are strictly modulated processes that markedly affect cellular functions<sup>34</sup>. *RAB13* has not been reported to be involved in the mechanism of macrophage polarization. Here we performed functional annotations for *RAB13* via GO terms and KEGG pathways, revealing that DEGs are mainly localized in collagen-containing extracellular matrix, spanning components of the plasma membrane, microvillus membrane, etc. In addition, involved biological processes were primarily responses to lipopolysaccharides, cell adhesion, immune system process regulation, etc. Molecular functions were mainly associated with chemokine activity and recipient binding, cytokine activity, etc. KEGG enrichment analysis demonstrated that enriched pathways were Cytokine-cytokine receptor interaction, Viral protein interaction with cytokine and cytokine receptor, Neuroactive ligand-receptor interaction, and ECM-receptor interaction signaling pathways. The central and peripheral nervous systems are also essential in regulating inflammation. Neuroactive ligand-receptor interaction affects the release<sup>35</sup> of *TNF- $\alpha$*  in sepsis-induced acute lung injuries. Previous studies reported that the ECM-receptor interaction signaling pathway is correlated with M2 macrophage polarization<sup>36</sup> with an unclear specific mechanism. Additionally, M1 macrophages can induce acute inflammatory responses and release pro-inflammatory cytokines (such as *IL-1 $\beta$* , *IL-6*, and *TNF- $\alpha$* ) and chemokines (including *CXCL5*, *CXCL9*, *CXCL10*, *CXCL11*, and *CXCL13*). In contrast, the M2 phenotype can produce anti-inflammatory factors (like *IL-10*) and is marked by specific markers *CD206* and *Arg1*, which are capable of reducing inflammation, promoting wound healing, and suppressing immunity. Overall, elevated *RAB13* levels positively correlate with the severity of sepsis patients and negatively correlate with survival rates. This may be associated with the inhibition of M1-like macrophage polarization, potentially involving mechanisms linked to the Neuroactive ligand-receptor interaction and ECM-receptor interaction signaling pathways. However, further research is needed to substantiate these underlying mechanisms<sup>37</sup>.

There are some limitations to this study. The sample size in this study is small, which may cause false positives. Selected patients were older than healthy volunteers, which might lead to compromised immunity. Cell experiments exploring molecular functions only had three groups, so errors were prone to occur. Cells that underwent sequencing were insufficient, and validation is required for the mechanism since the mechanism is inferred from sequencing data alone.

## Data availability

The datasets generated are available in the China National GeneBank DataBase (CNGBdb) repository and can be found below: <https://db.cngb.org/>, under the accession: CNP0002611, you can access it now and it's valid forever.

Received: 19 December 2023; Accepted: 30 August 2024

Published online: 02 September 2024

## References

- Font, M. D., Thyagarajan, B. & Khanna, A. K. Sepsis and Septic shock-basics of diagnosis, pathophysiology and clinical decision making. *Med. Clin. N. Am.* **104**(4), 573–585 (2020).
- Vincent, J. L., Opal, S. M., Marshall, J. C. & Tracey, K. J. Sepsis definitions: Time for change. *Lancet* **381**(9868), 774–775 (2013).
- Chen, X., Liu, Y., Gao, Y., Shou, S. & Chai, Y. The roles of macrophage polarization in the host immune response to sepsis. *Int. Immunopharmacol.* **96**, 107791 (2021).
- Yang, W. *et al.* Maresin 1 protects against lipopolysaccharide/d-galactosamine-induced acute liver injury by inhibiting macrophage pyroptosis and inflammatory response. *Biochem. Pharmacol.* **195**, 114863 (2022).
- Graier, J. J., Haggadone, M. D., Sarma, J. V., Zetoune, F. S. & Ward, P. A. Induction of M2 regulatory macrophages through the beta2-adrenergic receptor with protection during endotoxemia and acute lung injury. *J. Innate Immun.* **6**(5), 607–618 (2014).
- Sahgal, P. *et al.* GGA2 and RAB13 promote activity-dependent  $\beta$ 1-integrin recycling. *J. Cell Sci.* <https://doi.org/10.1242/jcs.233387> (2019).
- Moissoglu, K. *et al.* RNA localization and co-translational interactions control RAB13 GTPase function and cell migration. *Embo J.* **39**(21), e104958 (2020).
- Leek, J. P., Hamlin, P. J., Wilton, J. & Lench, N. J. Assignment of the Rab13 gene (RAB13) to human chromosome band 12q13 by in situ hybridization. *Cytogenet. Cell Genet.* **79**(3–4), 210–211 (1997).
- Lindsay, L. A., Nasir, R. F., Dowland, S. N., Madawala, R. J. & Murphy, C. R. Rab13 and desmosome redistribution in uterine epithelial cells during early pregnancy. *Reprod. Sci.* **28**(7), 1981–1988 (2021).
- Marzesco, A. M. *et al.* The small GTPase Rab13 regulates assembly of functional tight junctions in epithelial cells. *Mol. Biol. Cell.* **13**(6), 1819–1831 (2002).
- Peng, Z. *et al.* Multi-omics analyses reveal the mechanisms of arsenic-induced male reproductive toxicity in mice. *J. Hazard. Mater.* **424**, 127548 (2022).
- Wang, H. *et al.* Rab13 sustains breast cancer stem cells by supporting tumor-stroma cross-talk. *Cancer Res.* **82**(11), 2124–2140 (2022).
- Sun, J. *et al.* Exosomal miR-2276-5p in plasma is a potential diagnostic and prognostic biomarker in glioma. *Front. Cell Dev. Biol.* **9**, 671202 (2021).
- Wang, L. W. *et al.* Epstein-barr virus subverts mevalonate and fatty acid pathways to promote infected B-cell proliferation and survival. *PLoS Pathog.* **15**(9), e1008030 (2019).
- Condon, N. D. *et al.* Macropinosome formation by tent pole ruffling in macrophages. *J. Cell Biol.* **217**(11), 3873–3885 (2018).
- Fan, Y. *et al.* Revealing potential diagnostic gene biomarkers of septic shock based on machine learning analysis. *BMC Infect. Dis.* **22**(1), 65 (2022).

17. Yang, D. *et al.* CircRNA\_0075723 protects against pneumonia-induced sepsis through inhibiting macrophage pyroptosis by sponging miR-155-5p and regulating SHIP1 expression. *Front. Immunol.* **14**, 1095457 (2023).
18. Udompornpitak, K. *et al.* Polymeric particle BAM15 targeting macrophages attenuates the severity of LPS-induced sepsis: A proof of concept for specific immune cell-targeted therapy. *Pharmaceutics* **15**(12), 2695 (2023).
19. Ji, H. *et al.* Inhaled pro-efferocytic nanozymes promote resolution of acute lung injury. *Adv. Sci. (Weinh.)* **9**(26), e2201696 (2022).
20. Zhou, F. *et al.* Kinsenoside attenuates osteoarthritis by repolarizing macrophages through inactivating NF-kappaB/MAPK signaling and protecting chondrocytes. *Acta Pharm. Sin. B* **9**(5), 973–985 (2019).
21. Luo, J. *et al.* Targeted inhibition of FTO demethylase protects mice against LPS-induced septic shock by suppressing NLRP3 inflammasome. *Front. Immunol.* **12**, 663295 (2021).
22. Tian, Y. *et al.* Screening of potential immune-related genes expressed during sepsis using gene sequencing technology. *Sci. Rep.* **13**(1), 4258 (2023).
23. Nokes, R. L., Fields, I. C., Collins, R. N. & Fölsch, H. Rab13 regulates membrane trafficking between TGN and recycling endosomes in polarized epithelial cells. *J. Cell Biol.* **182**(5), 845–853 (2008).
24. Sun, Y., Jaldin-Fincati, J., Liu, Z., Bilan, P. J. & Klip, A. A complex of Rab13 with MICAL-L2 and  $\alpha$ -actinin-4 is essential for insulin-dependent GLUT4 exocytosis. *Mol. Biol. Cell.* **27**(1), 75–89 (2016).
25. Su, W. *et al.* Identification of autophagic target RAB13 with small-molecule inhibitor in low-grade glioma via integrated multi-omics approaches coupled with virtual screening of traditional Chinese medicine databases. *Cell Prolif.* **54**(12), e13135 (2021).
26. Zhang, X. D. *et al.* Clinical implications of RAB13 expression in pan-cancer based on multi-databases integrative analysis. *Sci. Rep.* **13**(1), 16859 (2023).
27. Yeo, J. C., Wall, A. A., Luo, L. & Stow, J. L. Sequential recruitment of Rab GTPases during early stages of phagocytosis. *Cell Logist.* **6**(1), e1140615 (2016).
28. Liu, Y. C., Zou, X. B., Chai, Y. F. & Yao, Y. M. Macrophage polarization in inflammatory diseases. *Int. J. Biol. Sci.* **10**(5), 520–529 (2014).
29. Mosser, D. M. & Edwards, J. P. Exploring the full spectrum of macrophage activation. *Nat. Rev. Immunol.* **8**(12), 958–969 (2008).
30. Orecchioni, M., Ghosheh, Y., Pramod, A. B. & Ley, K. Macrophage polarization: Different gene signatures in M1(LPS+) vs. classically and M2(LPS-) vs alternatively activated macrophages. *Front. Immunol.* **10**, 1084 (2019).
31. Li, Z. L. *et al.* Naringin improves sepsis-induced intestinal injury by modulating macrophage polarization via PPARgamma/miR-21 axis. *Mol. Ther. Nucleic Acids* **25**, 502–514 (2021).
32. Izadi, D. *et al.* Identification of TNFR2 and IL-33 as therapeutic targets in localized fibrosis. *Sci. Adv.* **5**(12), y370 (2019).
33. Jin, G. L. *et al.* Koumine regulates macrophage M1/M2 polarization via TSPO, alleviating sepsis-associated liver injury in mice. *Phytomedicine* **107**, 154484 (2022).
34. Locati, M., Curtale, G. & Mantovani, A. Diversity, mechanisms, and significance of macrophage plasticity. *Annu. Rev. Pathol.* **15**, 123–147 (2020).
35. Zhang, J. *et al.* Deregulated RNAs involved in sympathetic regulation of sepsis-induced acute lung injury based on whole transcriptome sequencing. *BMC Genom.* **23**(1), 836 (2022).
36. Wu, R. X., Ma, C., Liang, Y., Chen, F. M. & Liu, X. ECM-mimicking nanofibrous matrix coaxes macrophages toward an anti-inflammatory phenotype: Cellular behaviors and transcriptome analysis. *Appl. Mater. Today* **18**, 100508 (2020).
37. He, S. *et al.* Nicotinamide mononucleotide alleviates endotoxin-induced acute lung injury by modulating macrophage polarization via the SIRT1/NF-kappaB pathway. *Pharm. Biol.* **62**(1), 22–32 (2024).

## Acknowledgements

We thank BGI for instructing RNA sequencing.

## Author contributions

W.L., D.C., Y.H., S.L., designed the study. Q.Z and D.C performed the bioinformatics analysis and interpretation of the data. X.L., S.L wrote the manuscript. Y.H revised the manuscript and gave final approval of the version to be published. All authors read and approved the final manuscript. All authors have accepted responsibility for the entire content of this manuscript and approved its submission.

## Funding

This work was supported by the Sichuan Science and Technology Department (Number: 2019JDPT0003); The Southwest Medical University research project, Grant/Award Number: 2021ZKQN092; The study was supported by Project of science and technology department of sichuan province (2022NSFSC1522). the Health Commission of Sichuan Province (Grant No. 20PJ138).

## Competing interests

The authors declare no competing interests.

## Ethics approval and consent to participate

The study was conducted in strict accordance with the rules of the Declaration of Helsinki. The study protocol has been approved by the ethics committee of the Affiliated Hospital of Southwest Medical University (Ethical Approval No. ky2018029). The Registration Number was ChiCTR1900021261.

## Informed consent

Informed consent was obtained from all individuals included in this study.

## Additional information

**Supplementary Information** The online version contains supplementary material available at <https://doi.org/10.1038/s41598-024-71771-y>.

**Correspondence** and requests for materials should be addressed to W.L. or Y.H.

**Reprints and permissions information** is available at [www.nature.com/reprints](http://www.nature.com/reprints).

**Publisher's note** Springer Nature remains neutral with regard to jurisdictional claims in published maps and institutional affiliations.

**Open Access** This article is licensed under a Creative Commons Attribution-NonCommercial-NoDerivatives 4.0 International License, which permits any non-commercial use, sharing, distribution and reproduction in any medium or format, as long as you give appropriate credit to the original author(s) and the source, provide a link to the Creative Commons licence, and indicate if you modified the licensed material. You do not have permission under this licence to share adapted material derived from this article or parts of it. The images or other third party material in this article are included in the article's Creative Commons licence, unless indicated otherwise in a credit line to the material. If material is not included in the article's Creative Commons licence and your intended use is not permitted by statutory regulation or exceeds the permitted use, you will need to obtain permission directly from the copyright holder. To view a copy of this licence, visit <http://creativecommons.org/licenses/by-nc-nd/4.0/>.

© The Author(s) 2024